Research Article

Apigenin Ameliorates Ochratoxin A-Induced Hepatotoxicity in Rats via Modulation of Nrf2 and Wnt/β-Catenin Signaling Pathways

Rania Magdy Tawfik[1]*, Alia Mohamed Mahmoud[1], Alshymaa Othman Hammam Ahmed[2], Basma A. Ibrahim[3], Manar Ali Elsayed[1]

[1]Forensic Medicine and Clinical Toxicology Department, Faculty of Human Medicine, Zagazig University, Zagazig, Egypt; [2]Human Anatomy and Embryology Department, Faculty of Human Medicine, Zagazig University, Zagazig, Egypt; [3]Medical Biochemistry and Molecular Biology Department, Faculty of Human Medicine, Zagazig University, Zagazig, Egypt.

Abstract | Ochratoxin A is one of the most prevalent contaminated mycotoxins, found in various foods and cereals, resulting in serious threats to human and animal health. There is a lack of globally established approaches for ochratoxin A detoxification. Apigenin is a naturally occurring flavonoid that retains advantages linked to antioxidant, anti-inflammatory, and tumor suppressive effects. Investigating the possible ameliorative properties of apigenin against the hepatic toxicity induced by ochratoxin A in experimental rats. Four groups (8 rats each) were randomly assigned: control, apigenin (APG), ochratoxin A (OCA), and APG+OCA groups. Biochemical, molecular, histopathological, immunohistochemical and morphometric investigations were assessed. APG administration improved hepatic function by restoring liver enzymes, albumin level, and hepatic histopathology. APG restored the redox balance as evidenced by malondialdehyde alleviation and increased hepatic superoxide dismutase and glutathione peroxidase activities. Moreover, APG mitigated inflammation by restoring hepatic TNF-α and IL6 activities. In addition, APG moderated Nrf2/HO-1 and Wnt/β-Catenin/Cyclin D1 signaling pathways as indicated by Nrf2/HO-1 upregulation and Wnt/β-Catenin/Cyclin D1 downregulation. Furthermore, APG upregulated E-Cadherin and downregulated alpha fetoprotein gene expression. APG alleviated fibrosis and proliferation, as evidenced by Masson trichrome and immunostaining data of PCNA, respectively. This study provided novel findings highlighting the ameliorative potential of APG against OCA- induced hepatic oxidative damage, inflammation and hepatocellular proliferative signaling mediated via Nrf2/HO-1 and Wnt/β-Catenin/Cyclin D1 pathways.

Keywords | Ochratoxin A, Hepatotoxicity, Nrf2/HO-1, Wnt/β-Catenin/Cyclin D1, PCNA, Apigenin

Received | November 08, 2025; **Accepted** | November 27, 2025; **Published** | December 13, 2025
***Correspondence** | Rania Magdy Tawfik, Forensic Medicine and Clinical Toxicology Department, Faculty of Human Medicine, Zagazig University, Zagazig, Egypt; **Email:** nonamagdiano@gmail.com
Citation | Tawfik RM, Mahmoud AM, Ahmed AOH, Ibrahim BA, Elsayed MA (2025). Apigenin ameliorates ochratoxin a-induced hepatotoxicity in rats via modulation of Nrf2 and Wnt/β-catenin signaling pathways. Adv. Anim. Vet. Sci., 13(12):2702-2715.
DOI | https://dx.doi.org/10.17582/journal.aavs/2025/13.12.2702.2715
ISSN (Online) | 2307-8316

INTRODUCTION

Ochratoxin A (OCA) is one of the most prevalent contaminated mycotoxins, detected in a wide range of foods, including grapes, cereals, coffee, cocoa, dried fruit, dried herbs, pistachios, and cooked nuts. Dietary consumption is considered the main route of OCA exposure, causing serious threats to human and animal health (EFSA, 2020). The main species liable for OCA production are *Aspergillus* and *Penicillium*, which are massively present in places with high humidity and temperature (Wang *et al.*, 2022). OCA was reported to induce nephrotoxicity,

hepatotoxicity, neurotoxicity, genotoxicity, embryotoxicity, teratogenicity, immunosuppression, and carcinogenicity (Więckowska *et al*., 2024). The International Agency for Research on Cancer categorized OCA as an impending carcinogen presented in the 2B group (IARC, 1993). The liver is one of the chief target organs in OCA poisoning. Reports revealed that even little amounts of OCA initiated hepatic pathological and functional changes (Yu *et al*., 2018). OCA toxicity results from its ability to resist both the physical and chemical processing of modern food preparations without degradation owing to its stability besides the slowing rates of its decomposition, elimination, and excretion, resulting in OCA accumulation in organs and producing fatal health effects (Park *et al*., 2019). The exact mechanism of OCA poisoning is oxidative stress resulting in lipid peroxidation, DNA injury, and cancer promotion (Więckowska *et al*., 2024).

Accordingly, various health organizations have confirmed guidelines indicating the maximum allowed levels of OCA in different foods because of its large spread and significant damaging effects. At 2020, the European Union applied further reductions in the maximum permissible levels of OCA in roasted coffee, dried fruit and herbs, some herbal infusions, bakery items, and pistachios, these data based on applied assessments directed by EFSA, and focused on the toxicological hazards linked with OCA exposure (EFSA, 2020). At present, there is a lack of globally established approaches for OCA detoxification. So, one of the recognized methods for OCA neutralization is the consumption of several bioactive compounds like flavonoids known to have dietary antioxidant effects, as they can neutralize free radicals and maintain the oxidative balance in the body (Longobardi *et al*., 2022).

Apigenin (APG), a natural flavonoid, was obtained from *Matricaria chamomilla*. It is found extensively in different fruits and vegetables such as celery, parsley, onion, garlic, chamomile, propolis, honey, oranges, thyme, and spices. APG has numerous therapeutic effects, antioxidant, anti-inflammatory, besides anticancer activities, without having observable harmful effects (Salehi *et al*., 2019). Previous studies revealed that APG had hepatoprotective, chemoprotective, and anti-genotoxic effects against several rat models of liver injury (Ali *et al*., 2017). APG can protect against methotrexate (Goudarzi *et al*., 2021) and acetaminophen-induced hepatic damage in rats through the antioxidant and anti-inflammatory impacts (Zhao et al., 2020). The antioxidant effect of APG was related to Nrf2/HO-1 signaling activation, attenuating oxidative damage. Also, APG has an anti-inflammatory effect via inhibiting the proinflammatory mediators (TNF-α, IL-6), suppressing the inflammatory cascade (Al-Amarat *et al*., 2022). Numerous studies reported the cancer inhibitory role of APG, as it can moderate the expression of critical signaling pathways involved in cancer promotion (Pandey *et al*., 2023). APG administration has a direct effect on Wnt/β-catenin network by suppression of Wnt and β-catenin gene expression in addition to their signaling effector, Cyclin D1 (Lin *et al*., 2017).

Through reviewing literature, we observed that the protective effect of APG on ochratoxin A-induced hepatotoxicity was still under investigation. Thus, the target of this research is to determine the role of APG against OCA-induced hepatotoxicity, focusing on its defensive effects against oxidative stress, inflammation, and hepatocellular proliferation through some hepatic biomarkers and molecular changes, besides the histopathological, immunohistochemical, and morphometric analysis in the rat model.

MATERIALS AND METHODS

Chemicals

Ochratoxin A ($C_{20}H_{18}ClNO_6$) was available as a white crystal clear odorless powder with purity ≥ 97% HPLC. CAS number: 303-47-9, and molar mass 403.8 g/mol. It was obtained from Sigma Chemicals Company, Cairo, Egypt.

Apigenin ($C_{15}H_{10}O_5$) was available as a yellow crystal clear odorless solid with purity ≥ 95% HPLC. CAS number: 520-36-5, and molar mass 270.2 g/mol. It was obtained from Sigma Chemical Company, Cairo, Egypt. Dimethyl sulfoxide (DMSO) 10% was obtained as a vehicle from Cairo Pharmaceutical Company, Egypt.

Experimental animals

This experiment was implemented on mature albino rats, ethically permitted via the ZU-IACUC Board (Zagazig Institutional Animal Care and Use Committee), code: (IACUC3F2192024). The current experiment has been executed compliant with ARRIVE strategies and fulfilled the National Institute of Health rules. This research has been conducted in Forensic Medicine and Clinical Toxicology, Medical Biochemistry, and Anatomy departments of the Zagazig Faculty of Medicine, Egypt.

Thirty-two healthy mature male rats, each (180-200 g) weight and about 12 ± 1 weeks old, were obtained from the Animal House of Zagazig University. Rats were retained in metallic cages (2 rats/cage) under the regular ambient conditions (12-hour dark/light phases at a temperature of 25±2°C and 50–70% moisture). Rats were nourished regularly on balanced food, ad libitum, and were adapted for 14 days before the start of this experiment.

Experimental design and animal grouping

Thirty-two rats were allocated at random, using computer

generated randomization, into four groups (eight rats each), as follows:

- Group I (Vehicle control group): Received 0.03% DMSO (1mL/100g BW/day) orally for 8 consecutive weeks.
- Group II (Apigenin (APG) group): Received APG (50 mg/kg/day) orally dissolved in 0.03% DMSO for 8 weeks consecutively. APG dose selection was based on the hepatoprotective dose-response findings, reported by Alamri (2024).
- Group III (Ochratoxin A (OCA) group): Received OCA (0.5 mg/kg/day) orally dissolved in 0.03% DMSO for 8 consecutive weeks. This dose corresponds to 1/40 of the oral LD50 for rats (the oral LD50 in male rats is 22 mg/kg) (EFSA, 2020; Purchase and Theron, 1968). Furthermore, the administered OCA dose was chosen based on previously published toxicological studies (Damiano *et al*., 2021; Stoev, 2020), demonstrating that this level induces measurable hepatotoxic changes without causing overt or lethal toxicity.
- Group IV (APG+ OCA group): Received APG concomitantly with OCA with the same doses, manner, and duration as Groups II and III.

All treatments were administered via oral gavage tube, daily for a duration of 8 weeks as a time-response relationship in accordance with Choudhary *et al*. (2025) to assess the potential sub-chronic toxicity of OCA (OECD, 2018) and its alleviation by APG in albino rats.

Blood sampling and tissue preparation

Upon completion of this experiment and after the last dose of treatments, rats were anesthetized using sodium pentobarbital (Kilkenny *et al*., 2010). Blood specimens were procured and then centrifuged for 15 min at 3000 rpm to extract the sera. Sequentially, rats were humanely euthanized via cervical dislocation, then their livers were cautiously dissected out rinsed with ice-cold 0.9% saline. To eliminate remaining blood, hepatic tissues were cleaned with cold 50 mM phosphate-buffered saline (PBS, pH 7.4), washed, and sectioned for further analysis. The right liver lobe was fixed in 10% neutral-buffered formalin for histopathological assessment, whereas the left lobe was homogenized in five mL ice-cold PBS, then centrifuged at 3000 rpm for 15 minutes at 4°C, and then the supernatant was aliquoted and well-preserved at –80°C for no longer than 4 weeks prior to subsequent biochemical and molecular analysis.

MATERIALS AND METHODS

Biochemical investigations

Hepatic function biomarkers assay

The manufacturer's guidelines were followed to assay the serum levels of alanine transaminase (ALT, REF: 263002), aspartate transaminase (AST, REF: 259002), and albumin (REF: 210001) using a semi-automated biochemical analyzer (Sunostik, China), the assay kits were supplied by Biotechnology-Spectrum Diagnostics (Cairo, Egypt).

Hepatic oxidative/antioxidant assay

After the homogenization of hepatic tissues, the resulting supernatants were utilized to evaluate superoxide dismutase (SOD) activity following Misra and Fridovich (1972) protocol (bio-diagnostic kit, Cat. No. SD 2521), glutathione peroxidase (GPx) activity according to Tapple (1978) method (bio-diagnostic kit, Cat. No. GP 2524), and malondialdehyde (MDA) activity based on the procedure outlined by Ohkawa *et al*. (1979) (bio-diagnostic kit, Cat. No. MD2529).

Hepatic pro-inflammatory cytokines assay

The manufacturer's guidelines were monitored to assay the levels of tumor necrosis factor alpha (TNF-α, Cat. N. MBS2507393) and interleukin-6 (IL-6, Cat. N. MBS012805) in liver tissue homogenates using commercially available rat-specific ELISA kits from MyBiosource, Inc., California, USA.

Gene expression assay by quantitative real-time PCR (QRT-PCR)

Total RNA was extracted from liver tissue homogenates by using GENEzol™ Reagent (Geneaid, Taiwan). QRT-PCR of nuclear factor erythroid 2-related factor 2 (Nrf2), heme oxygenase-1 (HO-1), heat shock protein 70 (HSP70), wingless-type MMTV integration site family member 3A (Wnt3a), catenin beta-1(β-Catenin), Cyclin D1, epithelial cadherin (E-Cadherin), and alpha-fetoprotein (AFP) were examined. The isolated RNA was evaluated spectrophotometrically for purity and concentration, with all samples exhibiting A260/A280 ratios between 1.8 and 2.1. RNA *integrity* was confirmed by agarose gel electrophoresis, which revealed distinct ribosomal bands. Subsequently, cDNA was manufactured using the TOPscript™ cDNA Synthesis Kit (Enzynomics, South Korea). Real-time PCR amplification was implemented with the miScript SYBR Green PCR Kit (Qiagen, Germany) under definite cycling conditions: Initial denaturation at 94°C for 2 min, followed by 40 cycles of 95°C (15 sec, denaturation), 60°C (30 sec, annealing), and 72°C (60 sec, extension). All reactions were performed in triplicate technical replicates. Gene expression levels were standardized to the housekeeping gene β-actin and analyzed using the $2^{-\Delta\Delta CT}$ method (Livak and Schmittgen, 2001). Primer sequences were presented in Table 1.

Histopathological investigation

Liver specimens from experimental rats were fixed in 10% neutral buffered formalin for 24 hrs. Ascending grades of

Table 1: Primers sequences.

Genes	Sequences (5'-3')	GenBank accession No.	Product length (bp)
Nrf2	F: CTCCTTAGACTCAAATCCCACCTT R: GGACAGATCACAGCCCTCAAT	NM_031789.3	163
HO-1	F: ATGAGGAACTTTCAGAAGGGTC R: GTGGGGCATAGACTGGGTT	NM_012580.2	130
HSP70	F: TGGCTTTCACCGATACCGAG R: GTCGTTGATCACGCGGAAAG	NM_001285703.1	167
Wnt3a	F: CATACAGCCCATCTGCCAC R: AATCCAGTGGTGGGTGGATA	NM_001414349.1	226
β-Catenin	F: CTGGTGAAAATGCTTGGT TCA R: ACTGCCATTTTAGCTCCTTCTTGA	NM_001904.4	101
Cyclin D1	F: TGGAGCCCCTGAAGAAGAG R: AAGTGCGTTGTGCGGTAGC	NM_171992.6	424
E-Cadherin	F: GCAGTTCTGCCAGAGAAACC R: AATCCTGCTTCCAGGGAGAT	NM_031334.1	315
AFP	F: TGGAGAAGTGCTCCCAGTCT R: GCAGTGGTTGATACCGGAGT	NM_012493.2	359
β-actin	F: GTGCTATGTTGCTCTAGACTTCG R: ATGCCACAGGATTCCATACC	NM_031144.3	174

Nrf2: nuclear factor erythroid 2-related factor 2, HO-1: heme oxygenase-1, HSP70: heat shock protein 70, Wnt3a: wingless-type MMTV integration site family member 3A, β-Catenin: catenin beta-1, Cyclin D1, E-Cadherin: epithelial cadherin, AFP: alpha-fetoprotein, F: forward, R: reverse.

ethanol were used as a dehydrating agent, followed by xylene as a clearing agent. After that, the tissues were impregnated in wax to obtain paraffin blocks. Using a microtome (Leica RM 2155-UK), 5 µm thick paraffin sections were obtained and then stained with hematoxylin and eosin. Additional hepatic sections were stained with Masson's trichrome for collagen deposit detection (Suvarna *et al*., 2018). Photomicrographs from all sections were captured by using a light microscope fitted with a digital camera (Leica DM500) to be examined for pathological alterations.

Immunohistochemical investigation

Hepatic paraffin sections were subjected to immunohistochemical staining according to Hsu *et al*. (1981) and manufacturing protocol using mouse monoclonal anti-proliferating cell nuclear antigen (anti-PCNA) antibody (PC10, ab29; abcam, UK). Sections were dewaxed, rehydrated, and stained using DAB chromogenic agent (Expose mouse and rabbit specific HRP/DAB kit, abcam, Cat. N. ab80436). Counterstaining by hematoxylin was performed. Photomicrographs were captured using a light microscope fitted with a digital camera (Leica DM500).

Morphometric analysis

Morphometric analysis of H and E sections

Morphometric investigation of central and portal vein diameters was estimated by using the open-source ImageJ software (version 1.41). Dimensions were taken at 10× magnifications in eight microscopic fields per section. The maximum and minimum diameters of central and portal veins were measured, and the mean values were calculated for each group (Masyuk *et al*., 2003).

Morphometric analysis of Masson's trichrome and immunohistochemical sections

Both Masson's trichrome- and immunohistochemically stained hepatic sections were evaluated morphometrically by using an image analyzer computer system. The mean area percentage of collagen fibers in Masson's trichrome-stained sections and the mean area percentage of PCNA immunoreactivity were estimated in five non-overlapped high-power fields (400× magnification) per group. These area percentages were quantitatively measured using ImageJ analysis software (Fiji ImageJ, version 1.51n, NIH, USA). The percentage of areas-stained green color (positive zones) in Masson's trichrome-stained slides and brown color (positive zones) in PCNA-stained slides was calculated consistent with Varghese *et al*. (2014).

Statistical analysis

Data was analyzed using a one-way analysis of variance (ANOVA) test followed by post hoc analysis conducted using Tukey-Kramer methods in GraphPad Prism 8.0 software. Quantitative variables were defined through their means and standard deviations (SD). If the $(p < 0.05)$, the result was regarded as statistically significant, whereas $(p < 0.001)$, was regarded as highly significant.

Table 2: Effects of ochratoxin A and apigenin on hepatic function, oxidative stress and pro-inflammatory cytokines levels.

Variable	Control group (n=8)	Apigenin group (n=8)	Ochratoxin A group (n=8)	Apigenin + Ochratoxin A group (n=8)	p-value (ANOVA)
			Mean±SD		
ALT (U/L)	45.18±0.92	45.34±0.75	104.17±1.46[a]	49.60±3.86[b, c]	<0.001
AST (U/L)	117.03±1.74	116.84±1.85	190.05±2.73[a]	121.78±1.37[b, c]	<0.001
Albumin (g/dL)	3.74±0.35	3.81±0.45	2.18±0.13[a]	3.12±0.06[b, c]	<0.001
SOD (U/g)	7.74±1.04	7.88±0.79	4.65±0.40[a]	6.67±0.25[b, c]	<0.001
GPx (U/g)	13.25±1.33	13.45±1.26	6.59±0.54[a]	11.37±0.41[b, c]	<0.001
MDA (nmol/g)	0.39±0.10	0.40±0.08	1.04±0.15[a]	0.53±0.12[c]	<0.001
TNF-α (pg/mL)	1216.39±38.45	1207.71±40.24	2170.66±52.93[a]	1316.61±83.96[b, c]	<0.001
IL-6 (pg/mL)	47.89±1.07	46.95±1.37	72.12±3.52[a]	50.42±3.81[c]	<0.001

Data presented as mean ± SD (n= 8 rats). Significant: $p<0.05$, highly significant: $p<0.001$ ([a]$p<0.001$ and [b]$p<0.05$ vs. control; [c]$p<0.001$ vs. Ochratoxin A-exposed rats). ALT: alanine transaminase, AST: aspartate transaminase, SOD: superoxide dismutase, GPx: glutathione peroxidase, MDA: malondialdehyde, TNF-α: tumor necrosis factor alpha, IL-6: interleukin-6.

RESULTS

Biochemical results

A highly significant difference was noticed among the studied groups regarding all the studied parameters. Yet, no significant difference was distinguished between the control and APG groups.

Hepatic function biomarkers

OCA exposure induced significant hepatic dysfunction, as evidenced by 2.3-fold and 1.6-fold increase in ALT and AST activities, respectively (both $p<0.001$ vs. control), accompanied by a 41.7% reduction in serum albumin levels ($p<0.001$ vs. control). APG co-treatment demonstrated remarkable hepatoprotective efficacy, significantly attenuating transaminase elevations (ALT: 52.4% reduction; AST: 35.9% reduction) and markedly improving albumin levels by 43.1% compared to OCA-exposed animals (all $p<0.001$). Notably, despite this significant improvement, ALT, AST, and albumin levels in the APG+OCA group remained significantly different from those in the control group ($p<0.05$), indicating a partial recovery (Table 2).

Hepatic oxidative stress biomarkers

OCA intoxication significantly compromised the hepatic antioxidant defense system, reducing SOD and GPx activities by 39.9% and 50.3%, respectively (both $p<0.001$ vs. control). APG co-treatment substantially ameliorated the OCA-induced deficit in these antioxidant enzymes, achieving 43.4% and 72.5% of SOD and GPx activities, respectively compared to OCA-exposed animals (both $p<0.001$). Concurrently, OCA exposure induced a 2.7-fold increase in MDA levels ($p<0.001$) vs. control, which was attenuated by 49% with APG intervention ($p<0.001$) compared to OCA-exposed animals (Table 2). Our outcomes supported the hepatoprotective efficacy and anti-oxidative influence of APG against OCA-triggered oxidative damage in hepatic tissues.

Hepatic pro-inflammatory biomarkers

OCA exposure triggered a robust inflammatory response, elevating hepatic TNF-α and IL-6 concentrations by 78.5% and 50.6% respectively, compared to controls (both $p<0.001$). APG co-treatment effectively suppressed this cytokine storm, reducing TNF-α by 39.3% and reducing IL-6 to levels that were not statistically different from the control ($p>0.05$) (30.1% reduction vs. OCA group, both $p<0.001$) (Table 2). Our outcomes supported the anti-inflammatory influence of APG against OCA-triggered inflammation in hepatic tissues.

Real-time PCR gene expression results

Our gene expression analysis revealed that OCA significantly suppressed the hepatic antioxidant, Nrf2 expression by 38.24% (0.63±0.07-fold vs. control, $p<0.001$). This suppression impaired downstream signaling, evidenced by 58.83% lowered HO-1 levels (0.39±0.03-fold) and 72.81% decreased HSP70 (0.25±0.04-fold) vs. control ($p<0.001$), indicating compromised cellular defenses against oxidative and proteotoxic stress. APG co-treatment effectively counteracted these effects, significantly elevated Nrf2 to (0.92±0.09-fold) (46% increase vs. OCA group, $p<0.001$), which subsequently reactivated the pathway. This was evidenced by significant increase in HO-1 to 0.77±0.12-fold (97.4% improvement vs. OCA group) and marked induction of HSP70 by 3.4-fold (0.86±0.06 vs. OCA group) ($p<0.001$) (Figure 1A-C). While Nrf2 and HSP70 values in the APG+OCA group were not statistically different from control ($p>0.05$), HO-1 expression remained statistically different ($p<0.05$), demonstrating a strong but partial restoration of this specific antioxidant pathway.

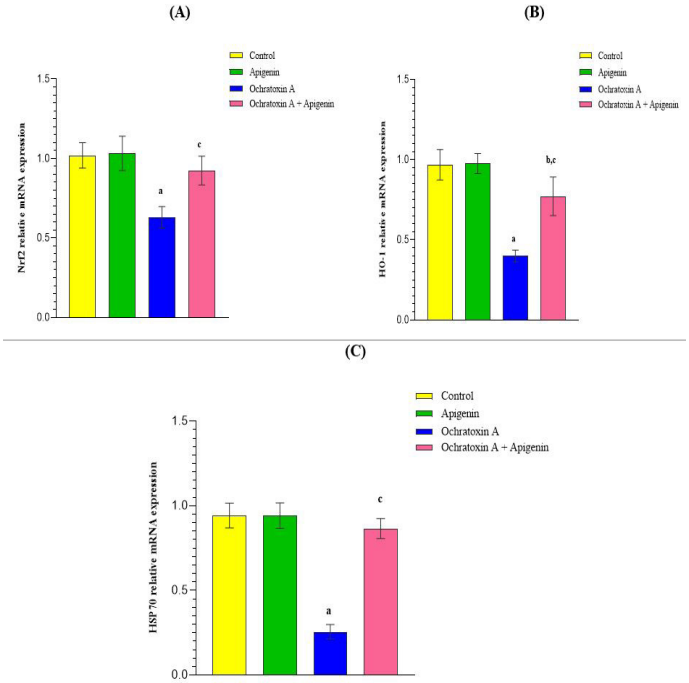

Figure 1: The effect of Ochratoxin A and Apigenin on hepatic Nrf2 (A), HO-1 (B), HSP70 (C) relative mRNA expressions across experimental groups in adult albino rats. Results expressed as mean ± SD (n=8), ([a]p<0.001 and [b]p<0.05 vs. control; [c]p<0.001 vs. Ochratoxin A-exposed rats), (ANOVA with Tukey's post hoc test). Nrf2: nuclear factor erythroid 2-related factor 2, HO-1: Heme oxygenase-1, HSP70: Heat shock protein 70.

Also, quantitative analysis of liver homogenates revealed that OCA exposure significantly increased Wnt3a ligand expression (4.32±0.06-fold vs. control, p<0.001), indicating activation of the Wnt signaling pathway. This induction was markedly attenuated by APG co-treatment, which reduced Wnt3a levels by 60.4% (1.71±0.17-fold, p<0.001 vs. OCA group) (Figure 2A). Consistent with Wnt pathway activation, OCA exposure led to a 3.1 ±0.34-fold increase in downstream of Wnt signaling, β-catenin mRNA (p<0.001 vs. control). APG co-treatment significantly reduced β-catenin mRNA by 52.7% (1.51±0.43-fold, p<0.001 vs. OCA group) (Figure 2B). Associated with β-catenin upregulation, we observed transcriptional activation of cell cycle regulator Cyclin D1 (3.82±0.16-fold, p<0.001 vs. control) concurrent with suppression of adhesion molecule E-cadherin (0.54±0.09-fold, p<0.001 vs. control). APG intervention effectively counteracted these changes, reducing Cyclin D1 expression by 56.8% (1.65±0.33-fold) and significantly increased E-cadherin to 0.90±0.12-fold (66.7% recovery, both p<0.001 vs. OCA group) (Figure 2C, D). The Wnt/β-catenin activation cascade ultimately elevated expression of hepatic AFP, a diagnostic marker for hepatocellular carcinoma, by 2.45±0.23-fold (p<0.001 vs. control). APG co-treatment significantly attenuated the OCA-induced elevation of AFP, reducing AFP levels by 46% (1.32±0.16-fold, p<0.001 vs. OCA group) (Figure 2E). Collectively, these findings demonstrate that APG provides a strong, multi-target protective effect by significantly ameliorating OCA-induced dysregulation of oncogenic signaling pathways. For the key genes (Wnt3a, β-catenin, Cyclin D1, and AFP), APG co-treatment brought expression levels much closer to the healthy control baseline but did not fully normalize them, as values in the APG+OCA group remained statistically different from the control group (p<0.05).

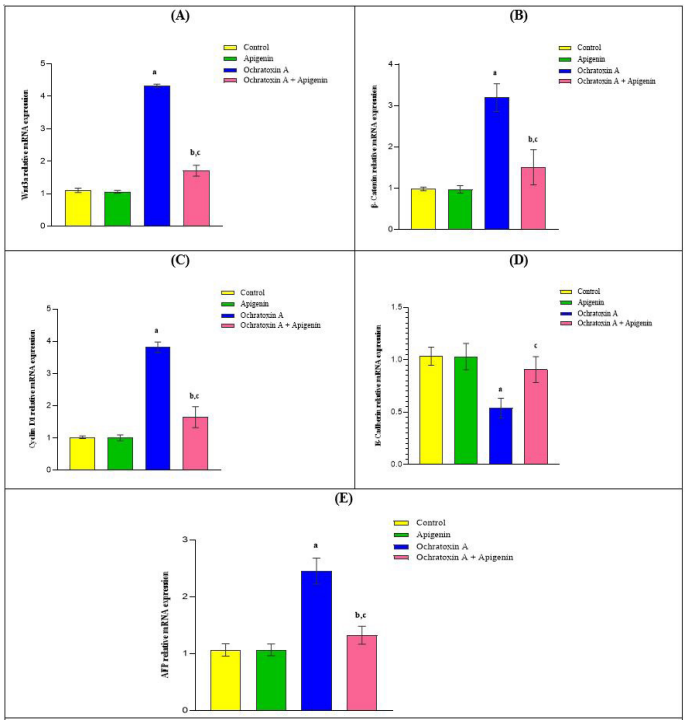

Figure 2: The effect of Ochratoxin A and Apigenin on hepatic Wnt3a (A), β-Catenin (B), Cyclin D1 (C), E-Cadherin (D), AFP (E) relative mRNA expressions across experimental groups in adult albino rats. Results expressed as mean ± SD (n=8), ([a]p<0.001 and [b]p<0.05 vs. control; [c]p<0.001 vs. Ochratoxin A-exposed rats), (ANOVA with Tukey's post hoc test). Wnt3a: wingless-type MMTV integration site family member 3A, β-Catenin: catenin beta-1, E-Cadherin: epithelial cadherin, AFP: alpha-fetoprotein.

Histopathological results of H and E-stained hepatic sections

Hepatic tissues of control (Figure 3A, F) and APG (Figure 3B, G) groups revealed normal histological structures of hepatic lobules which formed from plates of hepatocytes radiating from central vein and bordered by portal triad. The latter contained a branch of the hepatic artery, portal vein, and bile duct. The hepatocytes were polyhedral in shape with centrally located rounded vesicular nuclei. The hepatic sinusoids were located in between hepatocytes that lined by flat endothelial cells with Kupffer cells. While hepatic sections from OCA group (Figure 3C, D, H, I) exhibited loss of normal arrangement of hepatocytes with

multiple necrotic foci, inflamed portal areas, and intense congestion of portal vein. Also, focal areas of high degree of degenerated hepatocytes admixed with individual necrotic hepatocytes were observed. Mono nuclear inflammatory cell's infiltrations with dilated bile ducts were noticed. In contrast, the APG+OCA group demonstrated partial restoration with moderate histological improvement of hepatic parenchyma with few inflammatory cell's infiltration within portal area and slightly dilated congested portal vein were noticed (Figure 3E, J).

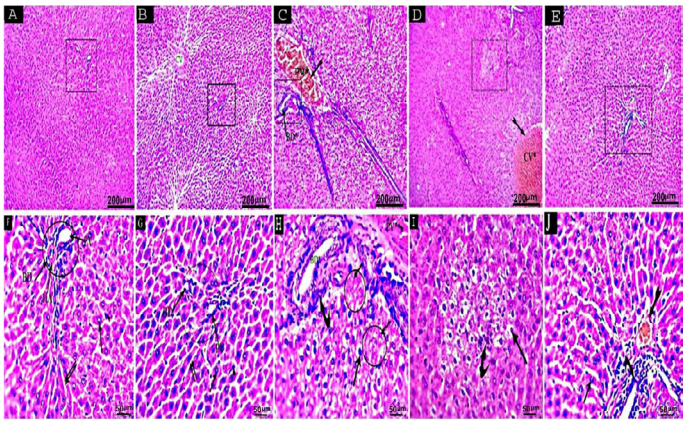

Figure 3: Photomicrographs of H&E-stained sections of rat liver in all experimental groups. (A and F) control and (B and G) apigenin groups showed normal histology of hepatocytes (black arrow), central vein (CV), sinusoids (double arrows), Kupffer cells (arrowhead) and portal triad (circle). The latter had branch of hepatic artery (HA), portal vein (PV), and bile duct (BD). (C, D, H and I) ochratoxin A group showed intense congestion of portal vein (PV*) (bifid arrow) and central vein (CV*). Focal areas of high degree of degenerated hepatocytes (arrow) admixed with unicellular necrotic hepatocytes and mono nuclear inflammatory cell infiltrates (curved arrow) and dilated bile duct (BD*) with loss of normal arrangement of hepatocytes and multiple necrotic foci (zigzag arrow) were also noted. (E and J) apigenin+ ochratoxin A group showed apparently normal hepatic parenchyma (arrow) with few inflammatory cell's infiltrations within portal area (curved arrow) and slightly dilated congested portal vein (bifid arrow). (H and E x 100, 400), Scale bar (500, 50μm).

Histopathological results of Masson's trichrome stained hepatic sections

Hepatic tissues of control (Figure 4A) and APG (Figure 4B) groups revealed few amounts of blue coloration for collagen fibres within vascular walls and portal areas. While the OCA group (Figure 4C) showed abundant areas of strong positive blue staining for collagen fibres. On the other hand, the APG+OCA group demonstrated moderate improvement with reasonable amount of blue staining of collagen bundles (Figure 4D).

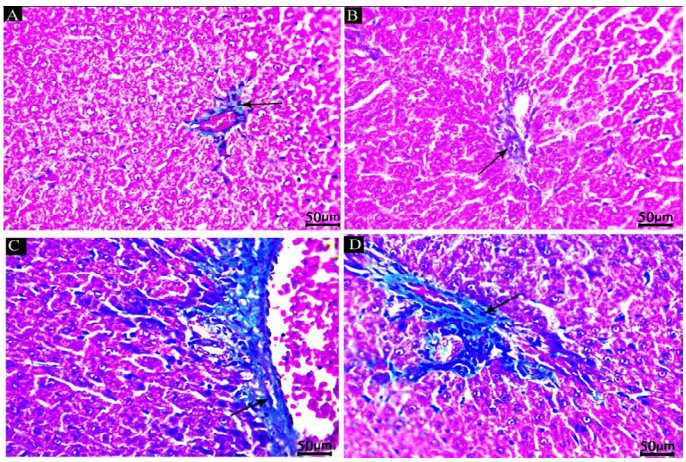

Figure 4: Representative photomicrographs of Masson trichrome stained sections of of rat liver showed blue stained areas for collagen fibres (arrows) within portal areas, and vascular walls in all experimental groups. (A) control and (B) apigenin groups showed low stainability for collagen fibres. (C) ochratoxin A group exhibited high stainability. (D) apigenin+ ochratoxin A group showed moderate stainability. (Masson trichrome x400, Scale bar, 50μm).

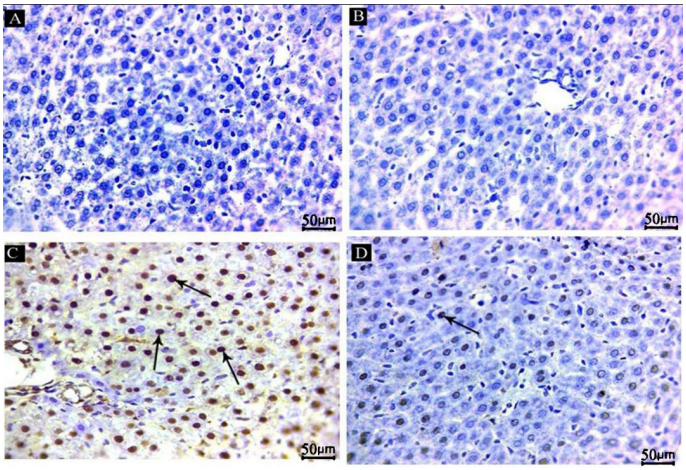

Figure 5: Demonstrative photomicrographs of immune-stained rat liver sections for PCNA expression. (A) control and (B) apigenin groups exhibited negative PCNA expressions in the cytoplasm of hepatocytes. (C) ochratoxin A group exhibited strong positive PCNA expression in the cytoplasm of hepatocytes with intense numbers of positive stained cells. (D) apigenin+ ochratoxin A group showed weak positive PCNA expression in the cytoplasm of hepatocytes with moderate numbers of labelled cells (the positive expressed cells revealed golden brown color). (PCNA immunostaining x400, Scale bar 50μm).

Immunohistochemical results

Regarding PCNA immuno-stained hepatic sections, the control (Figure 5A) and APG (Figure 5B) groups exhibited a negative PCNA immuno-expression in the nuclei of hepatocytes. However, in the OCA group, a strong positive PCNA immuno-expression was observed

in the nuclei of hepatocytes (Figure 5C). In contrast, the APG+OCA group exhibited moderate improvement with a weak positive PCNA immuno-expression in the nuclei of hepatocytes (Figure 5D).

Morphometric results

Morphometric results of H and E sections

A highly considerable difference was identified among the examined groups with respect to diameters of central and portal veins *(p<0.001)*. Post hoc analysis exhibited no significant difference between the control and APG group *(p>0.05)*. In the OCA group, a highly significant rise in both central and portal vein diameters was detected comparative to control *(p≤0.001)*. However, the APG+OCA group showed a highly significant reduction in these parameters relative to OCA group *(p<0.001)* but still there was a significant difference between the APG+OCA group and control group (*p<0.05*) (Table 3).

Morphometric results of Masson's trichrome sections

A highly significant difference was observed among the examined groups in the mean area percentage of Masson trichrome expression within the hepatic tissue (*p≤0.001*). Post hoc analysis exposed no remarkable differences between the control and APG group *(p>0.05)*. In the OCA group, a dramatic upsurge in area percentage of Masson trichrome expression was evident versus control *(p<0.001)*. Conversely, the APG+OCA group revealed a highly significant decline in this parameter when compared to OCA group *(p<0.001)* but still there was considerable difference between the APG+OCA group and control group (*p<0.05*) (Table 4).

Morphometric results of immunohistochemical sections

A highly significant difference among the examined groups in the mean area percentage of PCNA expression within the hepatic tissue (*p≤0.001*). Post hoc analysis displayed no remarkable differences between the control and APG group *(p>0.05)*. In the OCA group, a highly significant increase in area percentage of PCNA expression was detected when compared to control *(p<0.001)*. On the contrary, the APG+OCA revealed a highly significant decrease in this parameter when compared to OCA group *(p<0.001)* but still there was significant difference between the APG+OCA group and control group (*p<0.05*) Table 5.

DISCUSSION

Ochratoxin A, a mycotoxin produced by numerous *Penicillium* and *Aspergillus* species, signifies a considerable hazard to human health and animals due to its severe hepatotoxicity (Gao *et al*., 2022). OCA contaminates foodstuff and beverages, resulting in animal and human health issues. OCA poisoning can cause hepatic damage. Studies focused on the use of potentially protective compounds against OCA are insufficient (Więckowska *et al*., 2023). To further fill the gap in the search for potential

Table 3: Effects of ochratoxin A and apigenin on diameters of central and portal veins.

Variable	Control group (n=8)	Apigenin group (n=8)	Ochratoxin A group (n=8)	Apigenin+ Ochratoxin A group (n=8)	p-value (ANOVA)
	Mean±SD				
Diameters of central veins (µm)	43.80±1.92	41.23±1.41	105±13.7[a]	69.4±6.8[b, c]	>0.001
Diameters of portal veins (µm)	16.00±4.47	17.00 ±6.16	243.20±63.59[a]	75.40 ±19.92[b, c]	>0.001

Significant: p<0.05, highly significant: p<0.001, [a]*p*<0.001 and [b]*p*<0.05 vs. control; [c]*p*<0.001 vs. Ochratoxin A-exposed rats.

Table 4: Effects of ochratoxin A and apigenin on area % of Masson trichrome expression in hepatic tissues.

Variable	Control group (n=8)	Apigenin group (n=8)	Ochratoxin A group (n=8)	Apigenin+ Ochratoxin A group (n=8)	p-value (ANOVA)
	Mean±SD				
Area percentage of Masson trichrome expression	1.20 ± 0.447	1.60 ± 0.548	38.0±3.53[a]	11.4 ± 2.3[b, c]	> 0.001

Significant: p<0.05, highly significant: p<0.001, [a]*p*<0.001 and [b]*p*<0.05 vs. control; [c]*p*<0.001 vs. Ochratoxin A-exposed rats.

Table 5: Effects of ochratoxin A and apigenin on area % of PCNA expression in hepatic tissue.

Variable	Control group (n=8)	Apigenin group (n=8)	Ochratoxin A group (n=8)	Apigenin+ Ochratoxin A group (n=8)	p-value (ANOVA)
	Mean±SD				
Area percentage of PCNA expression	1.0± 0.707	0.60±0.548	37.20±7.12[a]	26.20± 6.87[b, c]	> 0.001

Significant: p<0.05, highly significant: p<0.001, [a]*p*<0.001 and [b]*p*<0.05 vs. control; [c]*p*<0.001 vs. Ochratoxin A-exposed rats.

drug therapies that can efficiently diminish the negative effects linked with OCA. This research was considered to examine the ameliorative efficacy of APG against OCA-induced hepatotoxicity in rats for the first time, with an emphasis on the molecular mechanisms by which APG exerts its beneficial effects.

Our findings revealed that OCA exposure markedly increased liver enzymes (ALT and AST) and reduced albumin levels, indicating substantial hepatic damage, consistent with Virk *et al.* (2020) and Damiano *et al.* (2021). This impairment of liver function is closely triggered by oxidative stress, a major cause of OCA toxicity (Liao *et al.*, 2024). Additionally, our study exhibited that OCA significantly elevated the lipid peroxidation biomarker (MDA) while simultaneously decreasing the antioxidant enzyme activity (SOD and GPx), hence corroborating the prooxidant influences of OCA. These data supported the accepted knowledge that OCA induced ROS release, resulting in hepatocyte damage as documented in the study performed by Alkuwayti (2025). Lipid peroxidation plays a major role in the carcinogenesis of variable hepatotoxic xenobiotics, recognized by marked upsurge in lipid peroxide level with a simultaneous decline in the enzymatic antioxidant level (Liu *et al.*, 2009). Opposing to our results, Marin *et al.* (2017a, b) observed that, in pigs, lower doses of OCA (50 µg/kg) augmented the SOD activity in the liver and kidney. This discrepancy may be caused by, species differences, as pigs and rats exhibit distinct metabolic rates and enzyme expression profiles. In addition, the OCA dose used by Marin *et al.* was lower than in our study. Also, exposure duration differed, with their study involving shorter-term treatment compared to our 8-week sub-chronic design, which could affect the antioxidant responses. Lastly, methodological differences in SOD estimation and tissue processing may contribute to this variation.

In a previous study, OCA induced renal oxidative stress, including the exhaustion of cellular antioxidant defenses. This oxidative stress has a crucial effect in provoking OCA-induced proliferative signaling linked with carcinogenic risk (Marin-Kuan *et al.*, 2011). In this study, gene expression analysis revealed that OCA significantly suppressed hepatic Nrf2 expression, impairing downstream antioxidant signaling as evidenced by reduced HO-1 levels. This result supported the previous studies by Shin *et al.* (2019) and Alkuwayti (2025), which recorded that OCA-induced oxidative stress was concomitant with the downregulation of Nrf2 and its downstream markers. The transcriptional factor Nrf2 obtains a crucial role in the cellular defense system against oxidative damage. Normally, it is sequestered in the cytoplasm by Keap1 and targeted for degradation. Conversely, upon exposure to free radicals or toxins, Nrf2 dissociates from Keap1, migrates to the nucleus, and binds to antioxidant response elements (ARE) in the specific target genes, stimulating the expression of various antioxidants, such as HO-1 (Liu *et al.*, 2022). The Nrf2/HO-1 pathway delivers multi-organ protection against numerous insults, mostly oxidative stress. It has an essential impact in regulating antioxidant, anti-inflammatory, and anti-proliferative mechanisms. Furthermore, multiple studies indicated that stimulation of the Nrf2/HO-1 axis might alleviate the progression of hepatic disorders (Li *et al.*, 2024). However, the results of Shin *et al.* showed that Nrf2 expression increased with extended OCA concentration. Additionally, enhanced expression of Nrf2 was observed in the nucleus rather than in the cytoplasm. This suggested that OCA might facilitate the migration of Nrf2 from the cytoplasm to the nucleus (Shin *et al.*, 2019). In the liver, OCA alters Nrf2 signaling in a time-and dose-dependent mode (Cavin *et al.*, 2007).

HSP70 is one of the heat shock proteins; it functions as a cell protein chaperon and acts as a sensor of redox changes. HSP70 contributed to protein refolding besides recovery of some proteins and elimination of irreversibly broken proteins. HSP70 could be considered as a biomarker of oxidative injury induced by mycotoxins (El-Golli Bennour and Bacha, 2011). In the current research, gene expression analysis revealed that OCA significantly suppressed hepatic HSP70 expression. This agrees with earlier studies of Barišić *et al.* (2002) and Klaric *et al.* (2014). On the contrary, an earlier study by Li *et al.* (2023) noticed the early upregulation of HSP70 expression in renal tissue after OCA exposure as a compensatory mechanism, and this may be a protective approach against biofunction impairment. HSP70 alleviated kidney injury via suppression of the JNK/MAPK cascade. However, prolonged OCA exposure with high doses could trigger HSP70 suppression (Li *et al.*, 2023). The liver is the target organ of numerous xenobiotics owing to its anatomical and physiological nature besides its crucial role in xenobiotic metabolism (Sturgill and Lambert, 1997). Free radicals cause hepatic structural and functional aberrations via the interaction with the hepatic cellular structures (Cichoz-Lach and Michalak, 2014).

In addition, OCA exposure caused a robust inflammatory response, elevating hepatic TNF-α and IL-6 levels, like the outcomes of Marin *et al.* (2018) and Alkuwayti (2025). During liver injury, inflammatory cells activate and release cytokines (TNF-α, IL-1β and IL-6), that cause neutrophils to accumulate in the liver and boost cytokine expression (Xu *et al.*, 2019). Furthermore, the development of hepatic neoplasms is an inflammation-based process such as chronic liver damage (Nakagawa and Maeda, 2012). Literature showed that mycotoxins, together with OCA, could trigger the release of pro-inflammatory marker TNF-α in rats (Xu *et al.*, 2019), and mild OCA poisoning caused severe systemic inflammatory reaction in pigs

(Bernardini *et al*., 2014).

In the existing study, gene expression analysis displayed that OCA significantly upregulated hepatic Wnt3a ligand expression, indicating activation of the Wnt signaling pathway. Consistent with this activation, OCA exposure also resulted in augmented expression of the downstream effector β-catenin mRNA, a finding comparable to that reported by Pyo *et al*. (2020) in renal tissues. Moreover, associated with β-catenin upregulation, we observed transcriptional activation of the cell cycle regulator Cyclin D1. Upregulation of Cyclin D1 enhanced abnormal proliferative signaling, which matched with the study of Chiu *et al*. (2003) on the acetaminophen hepatotoxicity model, and contributed to pre-neoplastic transformation, as also supported by Deane *et al*. (2001). Conversely, Aşcı Çelik *et al*. (2020) reported that OCA-induced downregulation of Cyclin D1 triggered cell cycle arrest, thereby preventing the propagation of damaged cells. Aberrant Wnt/β-catenin signaling deregulation has been related to several types of carcinogenic potentials. β-catenin is a main supplier of the Wnt pathway that stores in the cytoplasm then translocates to the nucleus, where it triggers downstream target genes to initiate cellular proliferation (Jia et al., 2016). In addition, in this work, we noticed suppression of the adhesion molecule E-cadherin. E-cadherin is an essential cellular adhesion protein that has crucial role in the maintenance of epithelial tissues (Xie et al., 2022). OCA induced endoplasmic reticulum stress and fibrosis observed by E-cadherin depletion in renal tissues (Yang *et al*., 2023). Moreover, deficits in E-cadherin adhesion are concomitant with the metastasis of invasive malignancies (Xie et al., 2022).

Our findings revealed raised expression of the hepatic AFP gene. An earlier study reported the increased levels of AFP in rats following consumption of aflatoxins (Hassaneen *et al*., 2023). AFP is a specific indicator for liver cancer. Aflatoxins increase the production of ROS, which damage DNA and result in carcinogenesis (Huang *et al*., 2020). In humans, Ibrahim *et al*. (2013) analyzed hepatocellular carcinoma (HCC) patients' serum to detect and quantify OCA. They reported that elevated OCA levels were frequently observed in the HCC group, with a five-fold elevation compared to the control group. Similarly, Rossi (2016) observed a higher incidence of HCC among cirrhotic patients who tested positive for OCA than in those with negative results. OCA may represent a major risk factor for tumors development in individuals with liver damage, which was consistent with experimental evidence that showed that OCA provoked ROS generation, activated the Wnt/β-catenin signaling network, and elicited tumorigenic propensity (Jia et al., 2016).

Thus, the observed activation of Wnt3a, β-catenin, and Cyclin D1, besides suppression of E-cadherin, in response to OCA exposure, suggests that OCA may promote liver injury not only through oxidative and fibrogenic pathways but also by engaging proliferative Wnt/β-catenin/Cyclin D1 signaling, thereby predisposing hepatocytes to molecular signatures indicative of early malignant risk.

Regarding the histopathological investigation in this study, OCA exposure provoked hepatic disarrangement with multiple necrotic foci, inflamed portal areas, and intense congestion of portal vein with dilated bile ducts were noticed, signifying obvious liver injury. Furthermore, collagen deposition was detected via Massons trichrome staining, signifying pronounced liver fibrosis. OCA increased PCNA immune expression in liver tissues indicating induction of cell proliferation. In an earlier study, Stoev (2020) described different types of hepatic neoplasia. The researcher mentioned one adenocarcinoma and one adenoma in the OCA group, while no neoplastic changes were detected in the control group.

Interestingly, our findings revealed that APG co-administration to rats exposed to OCA, significantly mitigated the adverse effects of OCA. APG markedly diminished the increased hepatic enzyme markers (ALT and AST), enhanced liver function, and mitigated oxidative stress. This is consistent with the results of Owui *et al*. (2023). Moreover, APG therapy augmented Nrf2 activation and the overexpression of HO-1 and enhanced HSP70 expression. These findings indicated that APG can help protect against OCA-induced hepatic damage by increasing the antioxidant capacity of the liver via activation of the Nrf2/HO-1 axis. This is attributed to the antioxidant behavior of APG, observed in the study of Al-Amarat *et al*. (2022). Many studies also highlighted that APG can display a protecting role against hepatic toxicity through boosting the ROS scavenging mechanisms (Goudarzi *et al*., 2021). APG co-treatment minimized the release of inflammatory cytokines, which is consistent with the results by Owumi *et al*. (2022).

In our findings, the co-administered APG appear to regulate cellular proliferation and tumor promoting signals by inhibiting Wnt/β-catenin expression and lowering the levels of cyclin D1 and AFP. In HCC, APG might inhibit tumor growth, promote tumor cells necrosis, and inhibit the expression of downstream linked genes by modulating miRNA expression (Peng *et al*., 2024). Similarly, APG inhibited the growth of hepatic cancer by modulation of Wnt/β-catenin signaling (Pan *et al*., 2021). APG was documented to target multiple pathways, such as Wnt/β-catenin, implicated in the progression of cancer (Fossatelli *et al*., 2023). APG inhibited HCC migration and invasion,

demonstrating that it could be a viable alternative therapy for intractable malignancies and offered potential as an anti-metastatic agent (Wang *et al*., 2024). Furthermore, in osteosarcoma, APG inhibited cellular proliferation by deactivation of Wnt/β-catenin cascade, thereby suppression of cell migration and invasion (Liu *et al*., 2015). The restoration of E-cadherin expression with APG co-treatment advocates stabilization of epithelial architecture. While these changes occur in pathways concomitant with metastatic inhibition in other studies (Oh *et al*., 2024), metastasis was not assessed in our 8-week sub- chronic toxicity model. Regarding AFP, a research implemented by Seydi *et al*. (2016) on liver cancer in a rat model reported the declined AFP levels following APG therapy, proposing the eligibility of the flavonoid APG as a complementary therapy for HCC patients.

In our study, the APG+OCA group revealed nearly normal liver architecture associated with a marked reduction of fibrous tissue deposition plus reduced cellular proliferation. This aligns with the research by Ji *et al*. (2021) and Melaibari *et al*. (2023). Furthermore, in prostate cancer xenograft models, APG inhibited PCNA expression, indicating suppression of the abnormal cellular proliferation, which was consistent with its anti-cancer and anti-fibrotic actions (Li *et al*., 2025). APG, a natural flavonoid, is thought to be effective in the prevention of human diseases triggered by oxidative stress and free radicals. APG is an antioxidant for the prevention of toxin-induced hepatic fibrosis (Xiang *et al*., 2018). APG has relatively potent anti-proliferative and anti-tumor effects on human cancer cell lines. The molecular mechanisms of action have been indicated as induction of apoptosis, DNA damage, and suppression of epithelial-mesenchymal transition (Li *et al*., 2025). APG therapy significantly reduced collagen accumulation, illustrating its capacity to inhibit OCA-induced fibrosis. This finding was consistent with research that showed that Nrf2 activation could alleviate fibrosis by inhibiting oxidative stress damage and preventing the activation of hepatic stellate cells (Hao *et al*., 2022). Although APG co-administration significantly attenuated OCA-induced molecular and histopathological changes, some parameters remained altered compared to controls. Therefore, it may reflect partial mitigation of toxicity rather than complete prevention of hepatotoxicity.

Limitation of the study

The present study provides strong correlative evidence for the involvement of Nrf2/HO-1 and Wnt/β-catenin pathways in the ameliorative effects of APG against OCA-induced hepatotoxicity. It is important to note that the established associations, while robust, are based on a model of co-administration and gene expression analysis. Confirming a direct causal relationship would require further investigative approaches, such as the use of specific pathway inhibitors or genetic modulations. Additionally, the 8-week sub-chronic design was instrumental in identifying early proliferative and pre-neoplastic molecular signatures; however, a longer-term study would be necessary to observe the full progression to carcinogenesis.

CONCLUSION

Briefly, the findings of this work provide convincing evidence that APG ameliorates OCA-induced hepatic injury in albino rats. These ameliorative benefits are associated with modulating the Nrf2/HO-1 and Wnt/β-catenin/Cyclin D1 signaling pathways, leading to reduction in oxidative stress, inflammation, hepatocellular proliferative signaling, and hepatic fibrosis. These outcomes suggest that APG may be a promising therapy for ameliorating hepatotoxicity induced by OCA exposure.

RECOMMENDATION

The clinical efficacy of APG against OCA should be investigated in various doses to explore the safety profile and optimal APG dosage as a potential adjuvant therapy in patients at risk of hepatotoxicity. Additionally, pathway perturbation experiments and long-term studies are warranted to determine whether the early protective effects of APG translate into significant prevention of liver injury or malignant progression.

ACKNOWLEDGMENT

The authors would like to express their appreciation to the animal house staff, Zagazig Faculty of Medicine, for their support and assistance.

NOVELTY STATEMENT

This study presents a comprehensive assessment of apigenin as an ameliorative agent against OCA-induced hepatotoxicity in rats. Through the integration of QRT-PCR based gene expression analysis with immunohistochemical and morphometric evaluations, this work establishes an innovative approach, highlighting the therapeutic potential of apigenin in mitigating hepatic insult.

AUTHOR'S CONTRIBUTION

RMT, AMM, BAI, MAE and AOHA: Conceptualization, data curation, formal analysis, funding acquisition, investigation, methodology, resources, software, supervision, validation, visualization, writing original draft, writing review and editing, project administration.

Generative AI and AI-assisted technology statement

The authors declare that the writing of this article did not utilize any AI software and technology.

Conflict of interest

The authors have declared no conflict of interest.

REFERENCES

Al-Amarat W, Abukhalil MH, Alruhaimi RS, Alqhtani HA, Aldawood N, Alfwuaires MA, Mahmoud AM (2022). Upregulation of Nrf2/HO-1 signaling and attenuation of oxidative stress, inflammation, and cell death mediate the protective effect of apigenin against cyclophosphamide hepatotoxicity. Metabolites, 12(7): 648. https://doi.org/10.3390/metabo12070648

Alamri ZZ (2024). Protective and therapeutic effects of apigenin on thioacetamide-induced hepatotoxicity in male rats: physiological and morphological study. Egypt Liver J., 14(1): 15. https://doi.org/10.1186/s43066-024-00318-7

Ali F, Rahul Naz F, Jyoti S, Siddique YH (2017). Health functionality of apigenin: A review. Int. J. Food Prop., 20(6): 1197-1238. https://doi.org/10.1080/10942912.2016.1207188

Alkuwayti MA (2025). Isoliquiritigenin attenuates ochratoxin A-induced hepatic oxidative stress and toxicity through the PI3K/AKT/Nrf2 pathway in Swiss albino mice. J. Bioch. Mol. Toxicol., 39(8): e70408. https://doi.org/10.1002/jbt.70408

Aşcı Çelik D, Gurbuz N, Toğay VA, Özçelik N (2020). Ochratoxin A causes cell cycle arrest in G1 and G1/S phases through p53 in HK-2 cells. Toxicon, 180: 11–17. https://doi.org/10.1016/j.toxicon.2020.03.012

B-Xie A, Maker AV, Priest DM, Dranow JN, Phan TE, Edwards BL, Staker PJ, Myler BM, Gumbiner S, Sivasankar S (2022). Molecular mechanism for strengthening E-cadherin adhesion using a monoclonal antibody. Proc. Natl. Acad. Sci. U.S.A. 119 (32): e2204473119. https://doi.org/10.1073/pnas.2204473119

Barišić K, Petrik J, Rumora L, Čepelak I, Grubišić TZ (2002). Expression of Hsp70 in kidney cells exposed to ochratoxin A. Arch. Toxicol., 76: 218–226.

Bernardini C, Grilli E, Duvigneau JC, Zannoni A, Tugnoli B, Gentilini F, Bertuzzi T, Spinozzi S, Camborata C, Bacci ML, Piva A, Forni L (2014). Cellular stress marker alteration and inflammatory response in pigs fed with an ochratoxin contaminated diet. Res. Vet. Sci., 97: 244–250. https://doi.org/10.1016/j.rvsc.2014.07.018

Cavin C, Delatour T, Marin-Kuan M, Holzhäuser D, Higgins L, Bezençon C, Guignard G, Junod S, Richoz-Payot J, Gremaud E (2007). Reduction in antioxidant defenses may contribute to ochratoxin A toxicity and carcinogenicity. Toxicol. Sci., 96: 30–39. https://doi.org/10.1093/toxsci/kfl169

Chiu H, Gardner CR, Dambach DM, Durham SK, Brittingham JA, Laskin JD, Laskin DL (2003). Role of tumor necrosis factor receptor 1 (p55) in hepatocyte proliferation during acetaminophen-induced toxicity in mice. Toxicol. Appl. Pharmacol., 193 (2): 218-227. https://doi.org/10.1016/j.taap.2003.07.003

Choudhary KG, Sharfuddin C, Kumar A, Ghosh AK (2025). Synergistic impact of aflatoxin and ochratoxin A exposure in charles foster rats: A toxicological study. Discov. Toxicol., 2(1): 1-18. https://doi.org/10.1007/s44339-025-00036-8

Cichoz-Lach H, Michalak A (2014). Oxidative stress as a crucial factor in liver diseases. World J. Gastroenterol., 20(25): 8082–8091. https://doi.org/10.3748/wjg.v20.i25.8082

Damiano S, Longobardi C, Andretta E, Prisco F, Piegari G, Squillacioti C, Montagnaro S, Pagnini F, Badino P, Florio S (2021). Antioxidative effects of curcumin on the hepatotoxicity induced by ochratoxin A in rats. Antioxidants, 10: 125. https://doi.org/10.3390/antiox10010125

Deane NG, Parker MA, Aramandla R, Diehl L, Lee WJ, Washington MK, Nanney LB, Shyr Y, Beauchamp RD (2001). Hepatocellular carcinoma results from chronic cyclin D1 overexpression in transgenic mice. Cancer Res., 61(14): 5389–5395.

EFSA Panel on Contaminants in the Food Chain (CONTAM), Schrenk D, Bodin L, Chipman JK, del Mazo J, Grasl- Kraupp B, Bignami M (2020). Risk assessment of ochratoxin A in food. EFSA J., 18(5): e06113. https://doi.org/10.2903/j.efsa.2020.6113

El-Golli-Bennour E, Bacha H (2011). Hsp70 expression as biomarkers of oxidative stress: Mycotoxins exploration. Toxicol., 287(3): 1-7. https://doi.org/10.1016/j.tox.2011.06.002

Fossatelli L, Maroccia Z, Fiorentini C, Bonucci M (2023). Resources for human health from the plant kingdom: the potential role of flavonoid apigenin in cancer counteractions. Int. J. Mol. Sci., 25(1): 251. https://doi.org/10.3390/ijms25010251

Gao YN, Wu CQ, Wang JQ, Zheng N (2022). Metabolomic analysis reveals the mechanisms of hepatotoxicity induced by aflatoxin m1 and ochratoxin A. Toxins, 14 (2): 141. https://doi.org/10.3390/toxins14020141

Goudarzi M, Kalantar M, Sadeghi E, Karamallah MH, Kalantar H (2021). Protective effects of apigenin on altered lipid peroxidation, inflammation, and antioxidant factors in methotrexate-induced hepatotoxicity. Naunyn Schmiedeberg's Arch. Pharmacol., 394: 523–531. https://doi.org/10.1007/s00210-020-01991-2

Hao W, Li M, Cai Q, Wu S, Li X, He Q, Hu Y (2022). Roles of NRF2 in fibrotic diseases: from mechanisms to therapeutic approaches. Front. Physiol., 13: 889792. https://doi.org/10.3389/fphys.2022.889792

Hassaneen NH, Hemeda SA, El Nahas AF, Fadl SE, El-Diasty EM (2023). Ameliorative effects of camel milk and silymarin upon aflatoxin B1 induced hepatic injury in rats. Sci. Rep., 13: 15092. https://doi.org/10.1038/s41598-023-41586-4

Hsu SM, Raine L, Fanger H (1981). Use of avidin-biotin-peroxidase complex (ABC) in immune peroxidase techniques: A comparison between ABC and unlabeled antibody (PAP) procedures. J. Histochem. Cytochem., 29(4): 577–580. https://doi.org/10.1177/29.4.6166661

Huang B, Chen Q, Wang L, Gao X, Zhu W, Mu P, Deng Y (2020). Aflatoxin B1 induces neurotoxicity through reactive oxygen species generation, DNA damage, apoptosis, and s-phase cell cycle arrest. Int. J. Mol. Sci., 21(18): 6517. https://doi.org/10.3390/ijms21186517

IARC (International Agency for Research on Cancer) monographs on the Evaluation of Carcinogenic Risks to

Humans (1993). Some naturally occurring substances: Food items and constituents, heterocyclic aromatic amines and mycotoxins; WHO; International Agency for Research on Cancer: Lyon, France, 1993. 56.

Ibrahim AS, Zaghloul H, Badria FA (2013). Case report evidence of relationships between hepatocellular carcinoma and ochratoxicosis. PLoS One, 8: e71423. https://doi.org/10.1371/journal.pone.0071423

Ji J, Yu Q, Dai W, Wu L, Feng J, Zheng Y, Li Y, Guo C (2021). Apigenin alleviates liver fibrosis by inhibiting hepatic stellate cell activation and autophagy via TGF-B1/SMAD3 and P38/PPAR*A* pathways. PPAR Res., 28: 6651839. https://doi.org/10.1155/2021/6651839

Jia X, Cui J, Meng X, Xing L, Shen H, Wang J, Liu J, Wang Y, Lian W, Zhang X (2016). Malignant transformation of human gastric epithelium cells via reactive oxygen species production and Wnt/β-catenin pathway activation following 40-week exposure to ochratoxin A. Cancer Lett., 372: 36–47. https://doi.org/10.1016/j.canlet.2015.12.007

Kilkenny C, Browne WJ, Cuthill IC, Emerson M, Altman DG (2010). Improving bioscience research reporting: The ARRIVE guidelines for reporting animal research. PLoS Biol., 8(6): e1000412. https://doi.org/10.1371/journal.pbio.1000412

Klarić MS, Medić N, Hulina A, Grubišić TZ, Rumora L (2014). Disturbed Hsp70 and Hsp27 expression and thiol redox status in porcine kidney PK15 cells provoked by individual and combined ochratoxin A and citrinin treatments, Food. Chem. Toxicol., 71: 97-105. https://doi.org/10.1016/j.fct.2014.06.002

Li H, He W, Yue D, Wang M, Yuan X, Huang K (2023). Low doses of fumonisin B1 exacerbate ochratoxin A-induced renal injury in mice and the protective roles of heat shock protein 70. Chem. Biol. Interact., 369: 110240. https://doi.org/10.1016/j.cbi.2022.110240

Li N, Hao L, Li S, Deng J, Yu F, Zhang J, Nie A, Hu X (2024). The NRF-2/HO-1 signaling pathway: A promising therapeutic target for metabolic dysfunction-associated steatotic liver disease. J. Inflamm. Res., 3(17): 8061-8083. https://doi.org/10.2147/JIR.S490418

Li X, Li Y, Chen S, Guo L, Mei N (2025). Potential anticancer effects and toxicity of flavones luteolin and apigenin *in vivo*. J. Environ. Sci. Health C Toxicol. Carcinog., 9: 1-37.

Liao C, Xu F, Yu Z, Ding K, Jia Y (2024). The Novel role of the NLRP3 inflammasome in mycotoxin- induced toxicological mechanisms. Vet. Sci., 11(7): 291. https://doi.org/10.3390/vetsci11070291

Lin CM, Chen HH, Lin CA, Wu HC, Sheu JJC, Chen HJ (2017). Apigenin-induced lysosomal degradation of β-catenin in Wnt/β-catenin signaling. Sci. Rep., *7*(1): 372. https://doi.org/10.1038/s41598-017-00409-z

Liu J, Qu W, Kadiiska MB (2009). Role of oxidative stress in cadmium toxicity and carcinogenesis. Toxicol. Appl. Pharmacol., 238(3): 209–214. https://doi.org/10.1016/j.taap.2009.01.029

Liu S, Pi J, Zhang Q (2022). Signal amplification in the KEAP1-NRF2-ARE antioxidant response pathway J. Redox. Biol., 54: 102389. https://doi.org/10.1016/j.redox.2022.102389

Liu X, Li L, Lv L, Chen D, Shen L, Xie Z (2015). Apigenin inhibits the proliferation and invasion of osteosarcoma cells by suppressing the Wnt/β-catenin signaling pathway. Oncol. Rep., 34: 1035–1041. https://doi.org/10.3892/or.2015.4022

Livak KJ, Schmittgen TD (2001). Analysis of relative gene expression data using real-time quantitative PCR and the 2(-Delta Delta C(T)) Method. Methods (San Diego, Calif.), 25(4): 402–408. https://doi.org/10.1006/meth.2001.1262

Longobardi C, Ferrara G, Andretta E, Montagnaro S, Damiano S, Ciarcia R (2022). Ochratoxin A and kidney oxidative stress: The role of nutraceuticals in veterinary medicine: A review. Toxins, 14(6): 398. https://doi.org/10.3390/toxins14060398

Marin DE, Braicu C, Gras MA, Pistol GC, Petric RC, Berindan Neagoe I, Palade M, Taranu I (2017a). Low level of ochratoxin A affects genome-wide expression in kidney of pig. Toxicon, 136: 67–77. https://doi.org/10.1016/j.toxicon.2017.07.004

Marin DE, Pistol GC, Gras M, Palade M, Taranu I (2018). A comparison between the effects of ochratoxin A and aristolochic acid on the inflammation and oxidative stress in the liver and kidney of weanling piglets. Naunyn-Schmiedeberg's Arch. Pharmacol., 391(10): 1147–1156. https://doi.org/10.1007/s00210-018-1538-9

Marin DE, Pistol GC, Gras MA, Palade ML, Taranu I (2017b). Comparative effect of ochratoxin A on inflammation and oxidative stress parameters in gut and kidney of piglets. Regul. Toxicol. Pharmacol., 89: 224–231. https://doi.org/10.1016/j.yrtph.2017.07.031

Marin-Kuan M, Ehrlich V, Delatour T, Cavin C, Schilter B (2011). Evidence for the role of oxidative stress in the carcinogenicity of ochratoxin A. J. Toxicol., 2011: 645361. https://doi.org/10.1155/2011/645361

Masyuk TV, Ritman EL, LaRusso NF (2003). Hepatic artery and portal vein remodeling in rat liver: vascular response to selective cholangiocyte proliferation. Am. J. Pathol., 162(4): 1175-1182. https://doi.org/10.1016/S0002-9440(10)63913-2

Melaibari M, Alkreathy HM, Esmat A, Rajeh NA, Shaik RA, Alghamdi AA, Ahmad A (2023). Anti-fibrotic efficacy of apigenin in a mice model of carbon tetrachloride-induced hepatic fibrosis by modulation of oxidative stress, inflammation, and fibrogenesis: A preclinical study. Biomedicines, 11(5): 1342. https://doi.org/10.3390/biomedicines11051342

Misra HP, Fridovich I (1972). The role of superoxide anion in the autoxidation of epinephrine and a simple assay for superoxide dismutase. J. Biol. Chem., 247(10): 3170-3175. https://doi.org/10.1016/S0021-9258(19)45228-9

Nakagawa H, Maeda S (2012). Inflammation- and stress-related signaling pathways in hepatocarcinogenesis. World J. Gastroenterol. 18(31): 4071–4081. https://doi.org/10.3748/wjg.v18.i31.4071

OECD (2018). Repeated dose 90-day oral toxicity study in rodents, OECD Guidelines for the Testing of Chemicals, Section 4, OECD Publishing, Paris.

Oh HM, Cho CK, Lee NH, Son CG (2024). Experimental evidence for anti-metastatic actions of apigenin: A mini review. Front. Oncol., 14: 1380194. https://doi.org/10.3389/fonc.2024.1380194

Ohkawa H, Ohishi N, Yagi K (1979). Assay for lipid peroxides in animal tissues by thiobarbituric acid reaction. Anal. Biochem., 95(2): 351–358. https://doi.org/10.1016/0003-2697(79)90738-3

Owumi SE, Ajakaiye B, Akinwunmi AO, Nwozo SO, Oyelere AK (2023). The hydrophobic extract of *Sorghum bicolor* (*L. moench*) enriched in apigenin-protected rats against aflatoxin B1-associated hepatorenal derangement. Molecules, 28(7):

3013. https://doi.org/10.3390/molecules28073013
Owumi SE, Kazeem AI, Wu B, Ishokare LO, Arunsi UO, Oyelere AK (2022). Apigenin-rich Sorghum bicolor (*L. moench*) extracts suppress A549 cells proliferation and ameliorate toxicity of aflatoxin B1-mediated liver and kidney derangement in rats. Sci. Rep., 12: 1–19. https://doi.org/10.1038/s41598-022-10926-1
Pan F, Zheng Y, Shi C, Zhang F, Zhang J, Fu W (2021). H19-Wnt/β-catenin regulatory axis mediates the suppressive effects of apigenin on tumor growth in hepatocellular carcinoma. Eur. J. Pharmacol., 893:73810. https://doi.org/10.1016/j.ejphar.2020.173810
Pandey P, Khan F, Upadhyay TK (2023). Deciphering the modulatory role of apigenin targeting oncogenic pathways in human cancers. Chem. Biol. Drug Des., 101(6): 1446-1458. https://doi.org/10.1111/cbdd.14206
Park S, Lim W, You S, Song G (2019). Ochratoxin A exerts neurotoxicity in human astrocytes through mitochondria-dependent apoptosis and intracellular calcium overload. Toxicol. Lett., 313: 42–49. https://doi.org/10.1016/j.toxlet.2019.05.021
Peng C, Zhang X, Zhou N, Hu T, Shen Y, Chen T, Liu Y, Cui H, Zhu S (2024). Apigenin inhibits lipid metabolism of hepatocellular carcinoma cells by targeting the histone demethylase KDM1A. Pytoey, 135: 156024. https://doi.org/10.1016/j.phymed.2024.156024
Purchase IFH, Theron JJ (1968). The acute toxicity of ochratoxin A to rats. Food Cosmet. Toxicol., 6(4): 479-483. https://doi.org/10.1016/0015-6264(68)90138-7
Pyo MC, Chae SA, Yoo HJ, Lee KW (2020). Ochratoxin A induces epithelial-to-mesenchymal transition and renal fibrosis through TGF-β/Smad2/3 and Wnt1/β-catenin signaling pathways *in vitro* and *in vivo*. Arch. Toxicol., 94(9): 3329–3342. https://doi.org/10.1007/s00204-020-02829-9
Rossi F (2016). Ochratoxin A and liver damage: A case-control study. EC Gastroenterol. Dig. Syst., 1: 66–75
Salehi B, Venditti A, Sharifi-Rad M, Kręgiel D, Sharifi-Rad J, Durazzo A, Martins N (2019). The therapeutic potential of apigenin. Int. J. Mol. Sci., 20(6): 1305. https://doi.org/10.3390/ijms20061305
Seydi E, Rasekh HR, Salimi A, Mohsenifar Z, Pourahmad J (2016). Selective toxicity of apigenin on cancerous hepatocytes by directly targeting their mitochondria. Anti-Cancer Agents Med. Chem., 16(12): 1576–1586. https://doi.org/10.2174/1871520616666160425110839
Shin HS, Lee HJ, Pyo MC, Ryu D, Lee KW (2019). Ochratoxin A-induced hepatotoxicity through phase I and phase II reactions regulated by AHR in liver cells. Toxins, 11(7): 377. https://doi.org/10.3390/toxins11070377
Stoev SD (2020). Long term preliminary studies on toxic and carcinogenic effects of individual or simultaneous exposure to ochratoxin A and penicillic acid in mice. Toxicon, 184: 192–201. https://doi.org/10.1016/j.toxicon.2020.06.013
Sturgill MG, Lambert GH (1997). Xenobiotic-induced hepatotoxicity: Mechanisms of liver injury and methods of monitoring hepatic function. Clin. Chem., 43(8): 1512–1526. https://doi.org/10.1093/clinchem/43.8.1512
Suvarna KS, Layton C, Bancroft JD (2018). Bancroft's theory and practice of histological techniques E-book, Elsevier health sciences: Amsterdam, The Netherlands.
Tapple AL (1978). Glutathione peroxidase and hydro-peroxidase. Methods Enzymol., 52: 506-513. https://doi.org/10.1016/S0076-6879(78)52055-7
Varghese F, Bukhari AB, Malhotra R, De A (2014). IHC Profiler: An open-source plugin for the quantitative evaluation and automated scoring of immunohistochemistry images of human tissue samples. PLoS One, 6; 9(5): e96801. https://doi.org/10.1371/journal.pone.0096801
Virk P, Al-Mukhaizeem NAR, Morebah SHB, Fouad D, Elobeid M (2020). Protective effect of resveratrol against toxicity induced by the mycotoxin, zearalenone in a rat model. Food Chem. Toxicol., 146: 111840. https://doi.org/10.1016/j.fct.2020.111840
Wang C, Feng X, Li W, Chen L, Wang X, Lan, Y, Tang R, Jiang T, Zheng L, Liu G (2024). Apigenin as an emerging hepatoprotective agent: current status and future perspectives. Front. Pharmacol., 15: 1508060. https://doi.org/10.3389/fphar.2024.1508060
Wang L, Hua X, Shi J, Jing N, Ji T, Lv B, Chen Y (2022). Ochratoxin A: Occurrence and recent advances in detoxification. Toxicon, 210: 11-18. https://doi.org/10.1016/j.toxicon.2022.02.010
Więckowska M, Szelenberger R, Niemcewicz M, Harmata P, Poplawski T, Bijak M (2023). Ochratoxin A-the current knowledge concerning hepatotoxicity, mode of action and possible prevention. Mol., 28(18): 6617. https://doi.org/10.3390/molecules28186617
Więckowska M., Cichon N., Szelenberger R., Gorniak L, Bijak M (2024). Ochratoxin A and its role in cancer development: A comprehensive review. Cancers, 16(20): 3473. https://doi.org/10.3390/cancers16203473
Xiang C, Teng Y, Yao C, Li X, Cao M, Li X, Pan G, Lu K, Galons H, Yu P (2018). Antioxidant properties of flavonoid derivatives and their hepatoprotective effects on CCl4 induced acute liver injury in mice. RSC Adv., 8: 15366–15371. https://doi.org/10.1039/C8RA02523A
Xie B, Maker A, Priest AV, Dranow DM, Phan JN, Edwards TE, Sivasankar S (2022). Molecular mechanism for strengthening E-cadherin adhesion using a monoclonal antibody. Proc. Natl. Acad. Sci., 119(32), e2204473119. https://doi.org/10.1073/pnas.2204473119
Xu W, Wang M, Cui G, Li L, Jiao D, Yao B, Xu K, Chen Y, Long M, Yang S, Hi J (2019). Astaxanthin protects ota-induced lung injury in mice through the Nrf2/NF-kappa B pathway. Toxins, 11: 540. https://doi.org/10.3390/toxins11090540
Yang SA, Rhee KH, Yoo HJ, Pyo MC, Lee KW (2023). Ochratoxin A induces endoplasmic reticulum stress and fibrosis in the kidney via the HIF-1α/miR-155-5p link. Toxicol. Rep., 10: 133-145. https://doi.org/10.1016/j.toxrep.2023.01.006
Yu Z, Wu F, Tian J, Guo X, An R (2018). Protective effects of compound ammonium glycyrrhizin, L arginine, silymarin and gluconolactone against liver damage induced by ochratoxin A in primary chicken hepatocytes. Mol. Med. Rep., 18: 2551–2560. https://doi.org/10.3892/mmr.2018.9285
Zhao L, Zhang J, Hu C, Wang T, Lu J, Wu C, Jiang Y (2020). Apigenin prevents acetaminophen-induced liver injury by activating the SIRT1 pathway. Front. Pharmacol., 11: 514. https://doi.org/10.3389/fphar.2020.00514